



Universiteit  
Leiden  
The Netherlands

## **Positional cloning in Xp22 : towards the isolation of the gene involved in X-linked retinoschisis**

Vosse, E. van de

### **Citation**

Vosse, E. van de. (1998, January 7). *Positional cloning in Xp22 : towards the isolation of the gene involved in X-linked retinoschisis*. Retrieved from <https://hdl.handle.net/1887/28328>

Version: Corrected Publisher's Version

License: [Licence agreement concerning inclusion of doctoral thesis in the Institutional Repository of the University of Leiden](#)

Downloaded from: <https://hdl.handle.net/1887/28328>

**Note:** To cite this publication please use the final published version (if applicable).

Cover Page



Universiteit Leiden



The handle <http://hdl.handle.net/1887/28328> holds various files of this Leiden University dissertation.

**Author:** Vosse, Esther van de

**Title:** Positional Cloning in Xp22 : towards the isolation of the gene involved in X-linked retinoschisis

**Issue Date:** 1998-01-07

## CHAPTER 2.1

### **An Xp22.1-p22.2 YAC contig encompassing the disease loci for RS, KFSD, CLS, HYP and RP15; refined localization of RS and KFSD**

Van de Vosse, E., Van der Wielen, M.J.R., Meershoek, E.J., Oosterwijk, J.C., Gregory, S.,  
Bakker, B., Weissenbach, J., Coffey, A.J., Van Ommen, G.J.B., and Den Dunnen, J.T.

Extended from:

*European Journal of Human Genetics* 4:101-104, 1996



## **An Xp22.1-p22.2 YAC contig encompassing the disease loci for RS, KFSD, CLS, HYP and RP15; refined localization of RS and KFSD.**

Esther van de Vosse, Michiel J.R. van der Wielen, Arthur A.B. Bergen, Eric J. Meershoek, Jan C. Oosterwijk, Simon Gregory, Bert Bakker, Jean Weissenbach, Alison J. Coffey, Gert-Jan B. van Ommen and Johan T. den Dunnen.

### **ABSTRACT**

Genetic linkage studies have mapped several diseases, including retinoschisis (RS), keratosis follicularis spinulosa decalvans (KFSD), Coffin-Lowry syndrome (CLS), X-linked hypophosphatemic rickets (XLH, locus name HYP) and X-linked dominant cone-rod degeneration (locus name RP15) to the Xp22-region. To facilitate the positional cloning of the genes involved, we have extended the molecular map of the region. Screening of several YAC-libraries allowed us to identify 63 Xp22 YACs, 52 of which localize between markers DXS414 (P90) and DXS451 (kQST80H1). Analysis of their marker content facilitated the construction of a YAC contig partially overlapping the existing map from the region and extending 1.5 Mb centromeric. The markers were ordered as follows: DXS414 - DXS987 - DXS207 - DXS1053 - DXS197 - DXS43 - DXS1195 - DXS418 - DXS999 - PDHA1 - DXS7161 - DXS443 - DXS7592 - DXS1229 - DXS365 - DXS7101 - DXS7593 - DXS1052 - DXS274 - DXS989 - DXS451. The region between DXS414 and DXS451 covers about 4.5 to 5 Mb, 1.5 Mb of which is in the newly mapped DXS1229-DXS451 region. Three additional markers (PDHA1, DXS7161 and DXS7592) were placed in the previously mapped region, thereby increasing the genetic resolution. Considering the known genetic distances, this region shows a significantly increased recombination frequency, of 0.2 Mb per cM. Using the deduced marker order, the analysis of key recombinants in families segregating RS allowed us to refine the critical region for RS to 0.6 Mb, between DXS418 and DXS7161. Similarly, the candidate region for KFSD could be limited to a 1 Mb region between DXS7161 and DXS1226.

### **INTRODUCTION**

To facilitate the isolation and study of disease genes, one has set out to completely characterize the human genome. This involves three main stages; mapping (both genetic and physical), cloning and sequencing. The first two steps are carried out in parallel and global physical and genetic maps have been published [1,2]. These crude maps subsequently require verification and refinement by detailed characterization of each region specifically. The human X chromosome is one of the best mapped human chromosomes and, at present, has the highest proportion of known markers and genes. Nonetheless, the Xp22.1-p22.2 region has a relative shortage of markers and is consequently bare in cloned genes [3]. On the other hand, linkage analysis mapped a number of disease loci to the Xp22.1-p22.2 region [4], including spondylo-epiphyseal dysplasia (SEDL, MIM 313400), retinoschisis (RS, MIM 312700), keratosis follicularis spinulosa decalvans (KFSD, MIM 308800), Coffin-Lowry syndrome (CLS, MIM 303600), X-linked hypophosphatemic rickets (XLH, locus name HYP, MIM 307800) and X-linked dominant cone-rod degeneration (locus name RP15, MIM 268000) [5]. Our group has a special interest in RS and KFSD. Linkage studies have placed the gene for RS, a rare hereditary vitreoretinal degeneration, between DXS43 and DXS365 [6,7]. Recently, we have shown that KFSD, a rare X-linked disorder characterized by follicular hyperkeratosis of the skin, scarring alopecia of the

scalp, absence of eyebrows and corneal degeneration, to be located between DXS16 and DXS269 [8]. Contiguous gene syndromes and large deletions, which have greatly contributed to the unravelling of other regions of the X chromosome, have not been reported in the Xp22.1-p22.2 region.

As a first step to resolve this lack of knowledge and towards identification of RS and KFSD, we have used known STS markers, *Alu*-PCR products of YACs isolated in the course of the project and new Généthon markers to screen YAC libraries and isolate YACs from the Xp22-region. An *Alu*-PCR-based fingerprinting method ([9], and Coffey *et al.* unpublished data) was used to assemble crude contigs and to determine overlaps between the YACs. Subsequently, we have used PCR and hybridization analysis to refine the contig, order the markers and construct a physical map. The deduced map spans about 4.5 to 5 Mb and includes the loci for RS, KFSD, CLS and HYP. While this work was ongoing, Alitalo *et al.* [10] published an Xp22-contig, which overlaps ours from DXS414 to DXS1229 and which is in complete agreement with the map we will present here. We place three additional markers (PDHA1, DXS7161 and DXS7592) in the overlapping region and our map extends at least 1.5 Mb proximally, spanning eight other markers. The mapping data were used to refine the localization of RS by linkage analysis to 0.6 Mb between DXS418 and DXS7161, and the localization of KFSD to 1 Mb between DXS7161 and DXS1226 [11].

## MATERIALS AND METHODS

### YAC library screening

YAC library screening was performed by hybridization. High-density gridded filters from the ICI library [12] and the X-specific subset of the CEPH megabase library ([13] and unpublished) were provided by the EU-sponsored YAC Screening Center Leiden (The Netherlands). Gridded *Alu*-PCR product filters from ICRF-library 900 [14] were provided by the ICRF (London, U.K.).

Filters were hybridized in 0.5 M Sodiumphosphate pH 7.2, 7% SDS, 1% BSA, 1 mM EDTA for 16 hours at 65°C. Filters were washed twice at RT in 40 mM Sodiumphosphate pH7.2, 0.1% SDS before scanning using a PhosphorImager (Molecular Dynamics). *Alu*-PCR products and cosmid probes were prehybridized with 100 µg sheared human placental DNA (Sigma) and 25 µg *Alu*-dimer DNA.

### Probes

Probes used for the YAC library screening included unique probes and cosmids containing markers known to be located in Xp22 and *Alu*-PCR products derived from positive YACs isolated in the course of the project. *Alu*-PCR products were generated using primer PDJ34 [15]. Probes used for detailed YAC analysis included *PvuII/BamHI* fragments of pBR322 to identify the pYAC4 vector arms, CRI-L1391 (DXS274) [16], P122 (DXS418) [17], pD2 (DXS43) [18] and PCR products derived from the markers listed in Table 1. Probes for the analysis of recombinant patient samples included, in addition to the markers used for YAC analysis, 782 (DXS85) [19], pXUT23 (DXS16) [20], C7 (DXS28) [21] and p99-6 (DXS41) [18].

### YAC analysis

Yeast clones were colony purified and high molecular weight DNA was isolated in LMT agarose plugs (Seaplaque, FMC) as described [22]. Initial characterization of YACs was performed by PFGE, FISH and PCR. *HindIII*-digested YACs were electrophoresed on 0.8% SeaKem LE

agarose gels.

### **Pulsed Field Gel Electrophoresis (PFGE)**

PFGE-analysis, using a CHEF-system, was performed under standard conditions [22]. Agarose gels (1%) in 45 mM Tris, 45 mM Boric acid, 0.5 mM EDTA, pH 8.3 were electrophoresed for 24 h at 180 V, with pulse times ranging from 20 to 70 s. Lambda oligomers and AB1380 yeast genomic DNA were used as size standards. After electrophoresis, gels were stained, photographed, blotted on Hybond-N<sup>+</sup> [22] and fixed by UV crosslinking. Filters were washed to 1x SSC at 65 °C before autoradiography.

### **Fluorescent In Situ Hybridization (FISH)**

FISH-experiments, including two-colour FISH, were performed according to Dauwerse *et al.* [23]. Total yeast DNA was labelled by nick translation in the presence of Dig-11-UTP and biotin-14-dATP and detected by FITC (green) and TRITC (red) respectively.

### **Polymerase Chain Reaction (PCR)**

PCR was carried out in a Perkin-Elmer Cetus thermal cycler in 30 µl reactions containing 50 mM Tris-HCl pH 9.0, 50 mM KCl, 1.5 mM MgCl<sub>2</sub>, 0.01% gelatin, 0.1% Triton X-100, 0.2 mM each dNTP, 0.2 mg/ml BSA, 25 pmol of each primer and 0.25 U *Taq* polymerase (Super*Taq*, HT Biotechnology) with 50 µl mineral oil overlay. An initial denaturation step of 5 min 94 °C was followed by 30 cycles of 94 °C 1 min, 50-65 °C (Table 1) 1 min, 72 °C 1 min. Products were separated on a 2% agarose gel.

PCR for linkage analysis in the RS families was performed in 15 µl reactions containing 150-210 ng DNA, 1.5 mM MgCl<sub>2</sub>, 10 mM Tris-HCl pH 9.0, 50 mM KCl, 0.01% gelatin, 0.1% Triton X-100, 0.2 mM dATP, 0.2 mM dGTP, 0.2 mM dTTP, 0.025 mM dCTP, 0.6 U Amplitaq<sup>TM</sup> (Cetus Inc), 0.27 pmol α<sup>32</sup>P-dCTP, 5 pmol of each primer with 50 µl mineral oil overlay. An initial denaturation step of 5 min 94 °C was followed by 30 cycles of 94 °C 1 min, 50 °C 1 min (or according to Table 1), 72 °C 2 min and a final step of 10 min 72 °C. Products were separated on a sequencing gel.

### ***Alu*-PCR fingerprint analysis**

Primary *Alu*-PCR was performed as described previously [9] using primers ALE1 and ALE3 together in a combined reaction [24]. A dilution of the primary PCR (Fig.1a) was used in a secondary PCR for 10 cycles in the presence of end-labelled ALE1 and ALE3. The products were run on a gel (Fig.1b) as described previously [25]. After autoradiography, the fingerprints were analyzed using the semi-automated gel scanning and analysis system used for the *C.elegans* cosmid fingerprinting project [26]. The positions and intensities of the products are compared and the probability of overlap between YACs is analyzed. In the resulting contig the length of a clone is depicted as the number of products it contains (Fig.1c).

### **Recombinants analysis**

For RS, linkage analysis has been carried out with at least six Xp22.2 markers in 21 families, 15 of which have been published previously [6,7]. From these studies, two families with key-recombination events were selected. DNA samples of 13 individuals from these two families were analyzed with 10 (family P 22.337) or 11 (family P 24.130) polymorphic markers.

Locus	Marker	Product size (bp)	T <sub>a</sub>	Reference
DXS414	P90	330	55	[27]
DXS987	AFM120xa9	206-224	55	[27]
DXS207	pPA4B	500	52	[27]
DXS1053	AFM164zd4	194-206	60	[2]
DXS197	pTS247	250	52	[27]
DXS43	pD2	86-130	55	[28]
DXS1195	AFM207zd6	235-239	56	[2]
DXS418	P122	140-158	58	[29]
DXS999	AFM234yf12	260-276	50	[27]
PDHA1	PDHA1	125	58	[27]
DXS7161	AFM291wf5	240-254	55	[4]
DXS443	pRX-324	204-210	50	[30]
DXS7592	AFMa244zg1	225-233	55	J.W.
DXS1229	AFM337wd5	202-230	56	[2]
DXS365	pRX-314	201-217	50	[30]
DXS7101	AFMa176zb1	156-164	55	J.W.
DXS7593	AFMa346zc1	209-223	55	J.W.
DXS1052	AFM163yh2	143-159	62	[31]
DXS989	AFM135xe7	173-199	50	[27]
DXS451	kQST80H1	182-204	55	[30]

**Table 1.** PCR markers used in the analysis.

T<sub>a</sub> = annealing temperature. J.W.= Jean Weissenbach (unpublished).

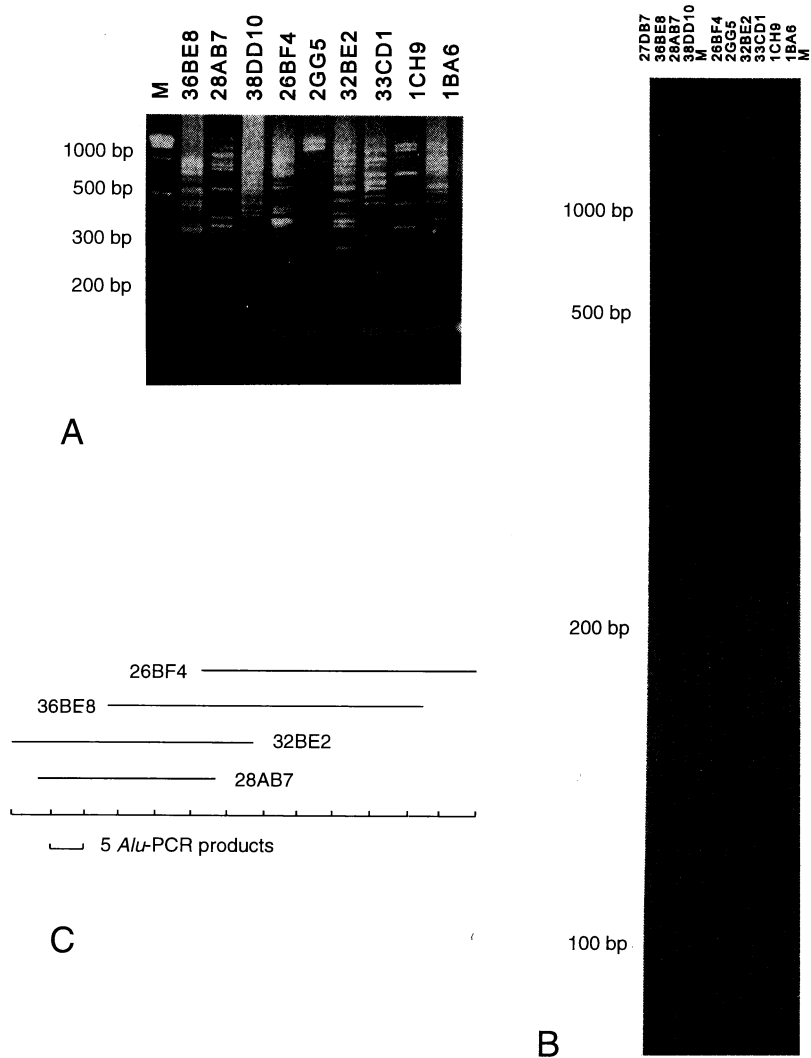


**Figure 1.** *Alu*-PCR fingerprinting. (A) 5  $\mu$ l of primary *Alu*-PCR products of 9 YAC clones run on a 2.5 % agarose minigel. Marker (M) is a 1 kb ladder. (B) Autoradiograph showing the *Alu*-PCR fingerprint of the 9 YAC clones. Marker (M) is a *Sau*3AI digested  $^{35}$ S-labelled lambda DNA marker. Sizes are indicated on the left of the autoradiograph. (C) Contig constructed after analysing the *Alu*-PCR bands using software originally written by J.Sulston for the *C.elegans* project [26].

## RESULTS

### YAC Library Screening

The CEPH [32], ICI [12] and ICRF [14,33] YAC libraries were screened with 21 probes which resulted in the isolation of 156 potential positive clones. To rapidly obtain a rough physical map, including potential overlap data, all 156 YACs were first *Alu*-PCR fingerprinted. An example of the *Alu*-PCR-based fingerprinting is shown in Fig. 1. YACs 36BE8, 28AB7, 26BF4 and 32BE2 share several bands (Fig. 1a and b) and therefore clearly overlap and form a contig (Fig. 1c). Analysis of all 156 YACs revealed the presence of ten *Alu*-PCR-based contigs, containing a total of 52 YACs. Four of these contigs, 13, 23, 25 and 82 (Fig. 2) were located in the Xp22.1-22.2 region as described below. The remaining 6 contigs were in other regions of the X chromosome and not further analyzed. Due to screening of the YAC library with *Alu*-PCR products of a chimeric YAC, contig 25 originally contained YACs that were located on chromosome 4 or 5 as deduced from FISH analysis.

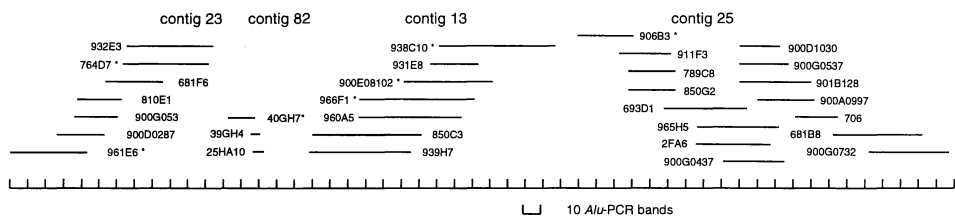


**Figure 2.** *Alu*-PCR fingerprinting contigs 13, 23, 25 and 82. The size of the clones is determined by the number of *Alu*-PCR bands it contains. An asterisk indicates YACs that give FISH-signals on Xp22 as well as on other chromosomes. Not all YACs in these contigs have been analyzed in detail.

### YAC analysis

Guided by the contigs derived from the fingerprinting, the YACs were tested for the presence of Xp22 markers. Out of the 156 YACs, 63 were positive for at least one marker, and 23 were positive for two or more markers. Since the density of YACs was high enough to construct a good contig, we only analyzed YACs containing two or more markers in greater detail and we did not analyze the 40 YACs containing only one marker. The remaining set of 93 YACs which were not positive for any of the markers, includes both false positives and YACs which, while located in an *Alu*-PCR contig, did not contain a reference marker.

The 23 YACs analyzed in detail ranged in size from 210 to over 1400 kb with an average size of 1050 kb (Table 2). The 19 CEPH YACs ranged in size from 590 to 1400 kb (1150 kb average), the 2 ICRF YACs were 580 and 1180/1300 kb (1020 kb average), and the 2 ICI YACs were 210 kb and 500 kb (380 kb average). These sizes do not differ significantly from those published (900 kb average for the CEPH library [32], 620 kb average for the ICRF library [14] and 350 kb average for the ICI library [12]). Sizes for specific YACs (Table 2) were usually consistent with available data (that is Généthon database [1] and [10]). One exceptional case was 939H7, which we find to be 1300 kb while it is reported as 270 kb in the database [1]. Since we performed a colony purification of the YAC clones it is possible that we have isolated the minor

component of a mixed YAC population. However, our data are consistent with those of Alitalo *et al.* [10] who report a length of 650 to 1500 kb and state that this YAC is unstable.

YAC	size (kb)	FISH
CEPH 961E6	1350 + >1400 (1680)	Xp22 + 4q + 16p
CEPH 810E1	1050 (1100)	Xp22
CEPH 681F6	950 (1060)	Xp22
CEPH 743A8	830 (700)	Xp22
ICI 40GH7	420 + 210	Xp22 + 6qcen
CEPH 764D7	N.A. (1420)	Xp22 + 8q1/2
CEPH 932E3	1280 (900)	Xp22
ICI 25HA10	430	Xp22
CEPH 811D11	1450 (800)	Xp22
CEPH 911F3	1150 (950)	Xp22
ICRF 900H0623	1180+1300	Xp22
CEPH 939H7	1300 (270)	Xp22
ICRF 900E08102	580	Xp22 + ( 3p )
CEPH 742H9	580 + 850 (1250)	Xp22
CEPH 966F1	950 (N.A.)	Xp22 + 19qtel
CEPH 960A5	1300 (1310)	Xp22
CEPH 850C3	590 (N.A.)	Xp22
CEPH 789C8	>1200 (1430)	Xp22
CEPH 850G2	1300 (1000)	Xp22
CEPH 693D1	1400 (1720)	Xp22
CEPH 965H5	1150 (1200)	Xp22
CEPH 681B8	930 (980)	Xp22
CEPH 933D5	900 (890) + 1450	Xp22 + 9ptel

**Table 2.** Detailed characterization of the YACs.

The YAC lengths as reported in the Généthon database are given between brackets. All YACs hybridized to Xp22, six YACs hybridized to other chromosomes as well. 900E08102 does not hybridize to #3 in all metaphases. YACs 742H9 and 960A5 were found to be non-chimeric by FISH, but have been found to be chimeric by Alitalo *et al.* [10] by analysis of YAC endclones. N.A.= not analyzed.

### FISH analysis

To verify the chromosomal localization of the YACs and to assess potential chimerism, we performed FISH analysis of all 23 YACs. Seventeen YACs showed a hybridization signal on Xp22 only, while six YACs gave more than one hybridization signal (Table 2). The CEPH data

of hybridizations of YAC-derived *Alu*-PCR products to gridded somatic cell hybrids confirm these data; 966F1 hybridizes to X and 18, 764D7 hybridizes to X and 8, 961E6 hybridizes to X, 10, 14, 16 and 18 and 933D5 hybridizes to X, 1 and 9. Two of the six, 900E08102 and 966F1, contained a single YAC as determined by PFGE and are thus most likely chimeric. Four clones contained more than one YAC. Since we performed a colony purification, they probably result from co-cloning of two different YACs in one yeast cell. Four YACs hybridized to Xp22 as well as to the heterochromatic regions on chromosome 1, 9 and 16. These YACs were not analyzed in detail because they did not contain more than one reference marker. However, this observation indicates that there is probably homology between Xp22 and these heterochromatic regions. Our data are not sufficient to localize this homology to a specific region within the contig.

For the ICI and ICRF YACs too few were studied to draw any significant conclusion about the chimerism frequency (ICRF less than 25% according to [34,35]). From the CEPH mega YACs only 2 out of 19 (11%) were chimeric. Alitalo *et al.* [10] analyzed YAC endclones and report chimerism in two more YACs (742H9 and 960A5). Small regions in YACs originating from other chromosomal regions are unlikely to be detected by FISH analysis which explains the differences observed.

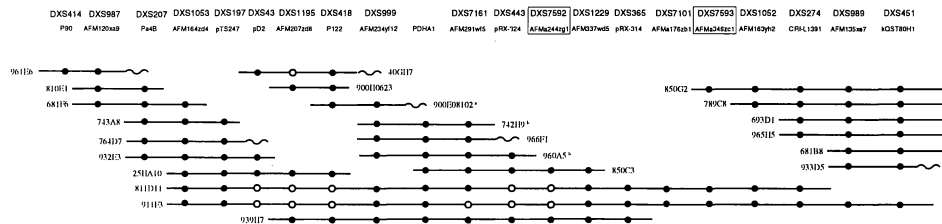


**Figure 3.** Marker based contig of the YACs. Closed circles indicate presence of the marker (after PCR or hybridization analysis), open circles indicate absence of the marker. Wavy lines indicate chimeric YACs. Multiplicity of YACs consistent with this order. Boxed markers are reagents additional to those previously located in contigs covering the region.

### YAC contig and marker order

Figure 3 shows the marker based contig of the YACs which could be constructed. YACs 961E6, 681F6, 25HA10, 939H7, 811D11 and 850G2 together span the entire region. Three YACs, 40GH7, 811D11 and 911F3, appear to contain internal deletions, since several markers were negative. In order to increase the marker density in the region and to locate markers which could not be ordered by genetic mapping, we tried to localize 18 new Génethon markers within the Xp22 region (Table 3). A first rough localization was achieved by testing on the somatic cell hybrids TG2sc1 [36] and AM445x393 [37]. TG2sc1 is a hamster hybrid containing Xp21.3-pter as the only human material, while AM445x393 contains Xp22.2-qter in a mouse background. DXS1223 and AFMa282vd1 were localized to Xp22.3 and fell outside our target region. Twelve markers located in the Xp21.3-p22.2 region, i.e. positive in both cell lines, were tested on the YACs from the contig. Five markers did not give discernable PCR products or gave inconclusive

data. We were able to localize DXS1195 between DXS418 and DXS43, DXS7161 between DXS443 and PDHA1, DXS1229 between DXS443 and DXS365, DXS7592 between DXS443 and DXS1229, DXS7101 between DXS365 and DXS1052, DXS1052 between DXS365 and DXS274, and DXS7593 between DXS7101 and DXS1052. DXS7105 is probably located between DXS365 and DXS7593 but only one YAC was positive with this marker (Table 3).

Marker	Total human	TG2sc1	AM445 x393	Localization	YAC results
DXS1028	+	-	-	? (not on X)	N.A.
DXS1043	+	+	+	Xp21.3-p22.2	no positives
DXS1052	+	+	+	Xp21.3-p22.2	see Figure 3
DXS1061	+	+	+	Xp21.3-p22.2	no positives
DXS1065	smear	-	+	(Xqtel-Xp21.3)	N.A.
DXS1195	+	+	+	Xp21.3-p22.2	see Figure 3
DXS1202	+	+	+	Xp21.3-p22.2	yeast also positive
DXS1223	+	+	-	Xp22.3	N.A.
DXS1224	-	-	-	?	N.A.
DXS1229	+	+	+	Xp21.3-p22.2	see Figure 3
DXS1233	-	-	-	?	N.A.
DXS7101	+	+	+	Xp21.3-p22.2	see Figure 3
DXS7105	+	+	+	Xp21.3-p22.2	811D11
DXS7161	+	+	+	Xp21.3-p22.2	see Figure 3
AFMa152xf1	-	400 bp	400 bp	?	N.A.
DXS7592	+	+	+	Xp21.3-p22.2	939H7, 850C3
DXS7593	+	+	+	Xp21.3-p22.2	see Figure 3
AFMa282vd1	+	+	-	Xp22.3	N.A.

**Table 3.** Localization of the new Généthon markers. TG2sc1 contains Xp21.3-pter as the only human material in a hamster background. AM445x393 contains Xqter-Xp22.2 in a mouse background. '+' = a product of the expected length was detected, '-' = no product of the expected length was detected. Between brackets; additional products or products with unexpected sizes amplified by the PCR.

### Candidate regions for KFSD and RS

The new data on the marker order generated was used to refine the localization of the candidate regions for RS and KFSD. For RS we have carried out linkage analysis with at least six Xp22.2 markers in 21 RS families, 15 of which have been published previously [6,7]. From these studies, two key-recombination events were identified, further refining the RS-gene candidate region (Fig. 4). In family P 22.337 the recombination between RS and DXS418, observed in patient III-3, places the disease gene proximal to DXS418. In family P 24.130, the recombination between RS and DXS7161 observed in patient III-3, places the disease gene distal to DXS7161. Unfortunately, DXS999 was not informative in this family.

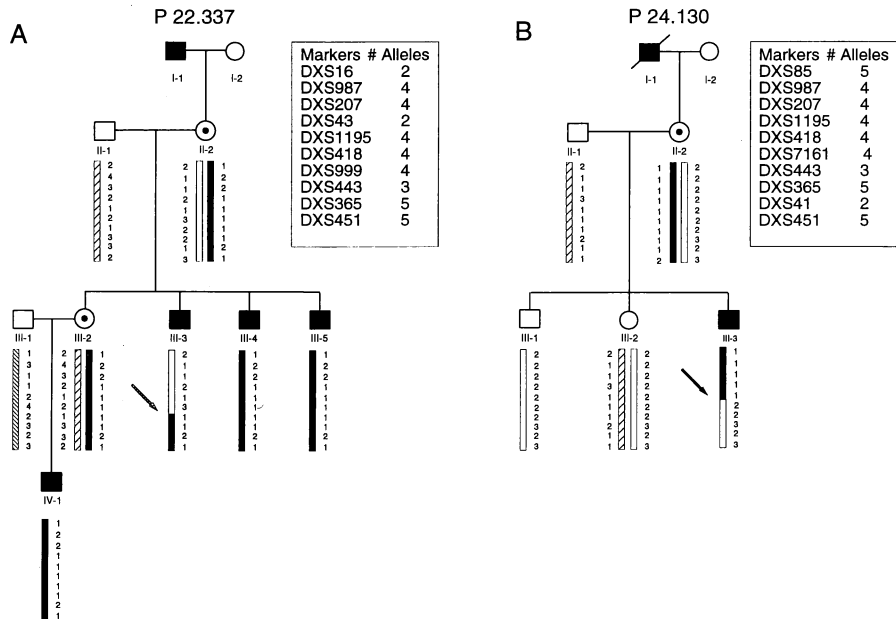


**Figure 4.** Refined critical region for RS. (A) In family P 22.337 the RS disease locus cosegregates, in general, with the haplotype 1 (DXS16) - 2 (DXS987) - 2 (DXS207) - 1 (DXS43) - 1 (DXS1195) - 1 (DXS418) - 1 (DXS999) - 1 (DXS443) - 2 (DXS365) - 1 (DXS451). The recombination observed with patient III-3, between RS and DXS16, DXS987, DXS207, DXS43, DXS1195 and DXS418, places the disease gene proximal to these loci. (B) In family P 24.130 the phase of the markers could be obtained through the analysis of the haplotypes of male III-1 and female III-2. Healthy male III-1 inherited the X-chromosome; 2 (DXS85) - 2 (DXS987) - 2 (DXS207) - 2 (DXS1195) - 2 (DXS418) - 2 (DXS7161) - 2 (DXS443) - 3 (DXS365) - 3 (DXS451) - 2 (DXS41) from his mother (II-2). The phase of the maternal X chromosomal alleles of female III-2 is also 2-2-2-2-2-2-2-3-2, since she inherited the X chromosome characterized by 2-1-1-3-1-1-2-1-1 from her father. Thus, patient III-3 is most likely recombinant for 2 (DXS7161) - 2 (DXS443) - 3 ((DXS365) - 2 (DXS41) - 3 (DXS451). The analysis of the recombination breakpoints in this family suggest the order Xpter-(DXS85, DXS987, DXS207, DXS1195, DXS418, RS) - (DXS7161, DXS443, DXS365, DXS41, DXS451) -Xcen. DXS999 was not informative.

For KFSD, recombinants were selected from a large Dutch pedigree Oosterwijk 1992[11]. Twenty polymorphic markers, 19 of which were informative, were tested (Fig. 5). Two individuals, VII-10 and VI-13 show key recombinations that refine the localization of the disease gene. VII-10, an affected male, determines the proximal border since the alleles of the affected chromosome recombine proximal to DXS257/DXS7161 with the healthy chromosome. VI-13, an affected male, determines the distal border by a recombination between DXS365 and DXS1229 [11].

TEL		VI-13	VII-10	
DXS85	782	●	○	
DXS16	pXUT23	—	○	
DXS987	AFM120xa9	●	○	
DXS43	pD2	●	—	
DXS418	P122	●	○	
DXS999	AFM234yf12	●	—	
DXS257	pQST1H3	●	○	
DXS7161	AFM291wf5	—	○	
DXS443	pRX-324	●	—	↑
DXS1229	AFM337wd5	—	—	KFSD
DXS365	pRX-314	●	●	↓
DXS1226	AFM316yf5	○	●	
DXS1052	AFMa163yh2	—	●	
DXS274	CRI L1391	○	—	
DXS989	AFM135xe7	○	●	
DXS451	kQST80H1	○	●	
DXS41	99.6	—	—	
DXS67	B24	—	—	
DXS28	C7	—	—	
DXS1235	STR50	—	●	
DXS1236	STR49	○	●	
DXS269	P20	○	●	
CEN				

**Figure 5.** Refinement of the localization of the critical region for KFSD. Family members, with a recombination in the Xp22-region, were selected from a large Dutch pedigree [11]. VI-13 and VII-10 are affected males.

### DISCUSSION

We have generated a contig map of Xp22.1-p22.2, thereby evaluating the use of two complementary methods: *Alu*-PCR fingerprinting and direct STS-content analysis of individual, overlapping YACs. Ultimately, the most informative data were obtained by testing specific markers directly on the individual YACs. However, the *Alu*-PCR fingerprinting method was found to be a fast and simple initial step to decrease the total workload allowing to divide the YACs into groups with overlapping sequences. The contigs derived by *Alu*-PCR fingerprinting are consistent with the contig based on marker content of the YACs. The four contigs generated on the basis of the fingerprinting alone were found to be all part of a single contig based on the STS content of the YACs. Similar results were obtained in a large chromosome 22 contig by

Coffey *et al.* (unpublished data). Chimerism of the YACs at the extremities of the contigs seems to play an important role. The gaps between contigs 23/82 and contigs 13/25 are both bordered by chimeric YACs, 764D7/40GH7 and 938C10/906B3 respectively. Furthermore, an overlap between a YAC that contains many *Alu*-PCR products and a YAC that contains only a few, will not be scored by the ContigC software used, since a 40% cut-off value of shared bands was used to determine overlap. This may explain why there is a gap between contigs 82 and 13, flanked by 25HA10 (producing 6 PCR-products) and 939H7 (producing 58 products).

*Alu* sequences are known to have a non-random distribution. Giemsa-positive bands -like Xp22.1- have a low *Alu*-repeat content [38]. The average number of *Alu*-PCR products of the YACs in our contig was 3.4 per 100 kb, varying from 1.2 to 10. Although our contig is supposed to span the Xp22.1/Xp22.2 border, we did not observe any significant differences in the number of *Alu*-PCR products derived from the YACs throughout the contig. However, we did observe a significantly decreased frequency of chimerism for the CEPH YACs isolated; 11% compared with the 40-50% chimerism reported [1]. Since a major cause of chimerism is probably recombination during the cloning step at homologous, mainly repetitive DNA sequences [39] the low frequency of chimerism in this region also indicates that it contains a lower number of highly repetitive DNA sequences.

### Marker order and physical distances

The marker order that was obtained, DXS414 - DXS987 - DXS207 - DXS1053 - DXS197 - DXS43 - DXS1195 - DXS418 - DXS999 - PDHA1 - DXS7161 - DXS443 - DXS7592 - DXS1229 - DXS365 - DXS7101 - DXS7593 - DXS1052 - DXS274 - DXS989 - DXS451 is in agreement with the consensus map of the 5<sup>th</sup> X-chromosome Workshop [4] and as published by Alitalo *et al.*[10]. Markers DXS443 and PDHA1, not separated previously [4], could be physically ordered by YACs 742H9 and 966F1, which both contain PDHA1 and DXS999, but not DXS443. Consequently, PDHA1 is distal to DXS443. Markers DXS7161, DXS7592, DXS7593 and DXS7101 were not physically mapped before.

Given that YACs are deletion prone and may rearrange, we have tested for the criterium that two or more YACs needed to be consistent with the derived marker position. This criterium applies for the entire contig (2-7 YACs multiplicity, average 4) except for the distal end and the interval DXS43-DXS1195 which was mapped independently by Alitalo *et al.* [10]. Combining the YAC marker content (Fig.3) and YAC length (Table 2) allows the construction of a physical map of the region (Fig 6). For example, YAC 25HA10 is relatively small (430 kb), indicating that the markers DXS1053-DXS418 map close to each other. 932E3 overlaps with 25HA10 and measures 1280 kb. Since only DXS1053-DXS43 are shared, 932E3 extends at least 850 kb to the telomeric side, a region which contains DXS207 (present in 932E3, absent in 25HA10). Similarly, the 830 kb YAC 743A8 extends in the same direction, although it misses DXS43. Combining the data of 810E1 and 681F6 leads to the conclusion that DXS987 is separated by about 900 kb from the start of a 400 kb cluster containing DXS1053, DXS197, DXS43, DXS1195 and DXS418, while DXS207 maps somewhere in between.

The combined data shows that the region between DXS414 and DXS451 measures 4.5 to 5 Mb (Fig.6). We were not able to determine the distance between DXS414 and DXS987, since only one chimeric YAC (961E6) was analyzed and since no markers telomeric of DXS414 were tested. The physical distances reported by Francis *et al.* [40] and Alitalo *et al.* [10], are in full agreement with the map presented here.

The ratio between physical and genetic distance is roughly 1 Mb/cM for the entire human genome. The available genetic data indicate that the Xp22.1-p22.2 region analyzed here has a highly increased recombination frequency (Fig.6). The estimated physical distances, in combination with the published genetic distances [31,41], give an average ratio of approximately 0.2 Mb/cM for the region between DXS987 and DXS989. This effect is more pronounced proximal to DXS1053 and reaches a peak value of 8 cM over 900 kb, about 1 cM per 100 kb, between DXS7161 and DXS1052.

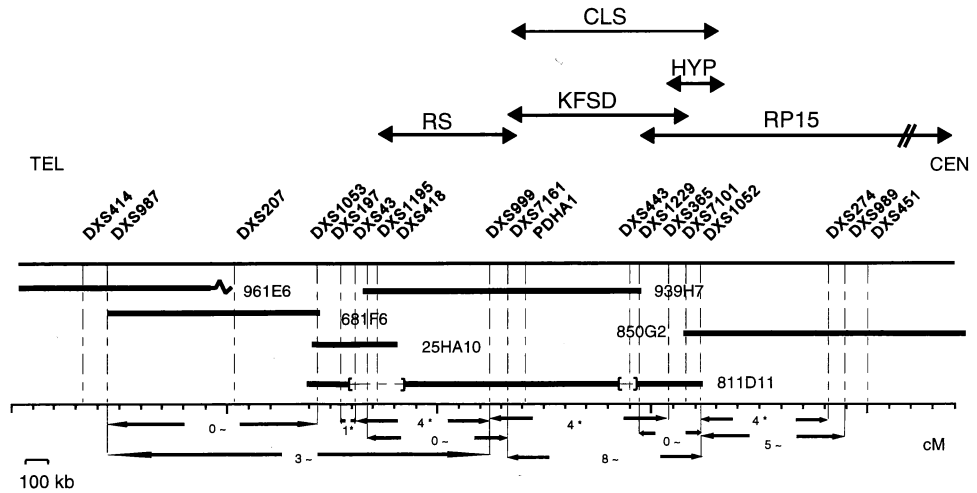


**Figure 6.** Physical map of the Xp22.1-p22.2 region. Physical map of the region obtained after combining marker content and length of all 23 YACs analyzed in detail. Only the YACs that form the minimal contig covering the entire region are shown. The indicated disease gene candidate regions are according to the 5<sup>th</sup> X-chromosome Workshop [4] and updated with the results published in this paper. The genetic distances (in cM) indicated at the bottom of the figure are according to ~Weissenbach *et al.* [41] and Francis *et al.* [40]

#### Disease gene candidate regions

The candidate regions for the HYP, CLS, RS, KFSD and RP15 disease genes are indicated in the physical map (Fig.6). The candidate region for HYP was localized between DXS365 and DXS274 by Francis *et al.* [40], a localization which was refined recently to between DXS365 and DXS1683 (a new marker between DXS365 and DXS1052) [4]. In our contig, this region measures less than 0.3 Mb. The CLS candidate region was first localized between DXS7161 and DXS1052 [42], a localization refined recently to between DXS7161 and DXS1683 [4], in our contig a region of approximately 1 Mb. The RP15 candidate region was localized between DXS1048 and DXS1229 by McGuire *et al.* [5].

The results presented here, combined with linkage data of Oosterwijk *et al.* [11], refine the localization of KFSD to less than 1 Mb between DXS7161 and DXS1226. The localization

of RS is refined to 0.6 Mb between DXS418 and DXS7161. Strikingly, and illustrating the relative underdevelopment of this region in terms of reagents, the limiting factor for each of these candidate regions to further refine the localization of the disease genes still is the lack of informative polymorphic markers rather than the absence of recombinants. The contig constructed allowed us to outline the specific requirements for a marker which will further narrow down the disease candidate regions. For instance in the case of KFSD, an informative marker between DXS7161 and DXS365 would be especially valuable and could potentially decrease the candidate region from 1 Mb to less than 200 kb. Similarly, the candidate region for RS now spans a 600 kb region devoid of any informative marker. Development of new polymorphic markers, based on the clones in the contig presented, is therefore a rewarding effort which we are currently undertaking. On the other hand, the candidate regions for the diseases mentioned have now become small enough to consider establishing a transcriptional map in order to isolate the gene(s) involved in these diseases.

### **ACKNOWLEDGEMENTS**

Gridded colony filters of the CEPH Mega-X library were provided by Denis Le Paslier and Ilya Chumakov at the Centre d'Etude du Polymorphisme Humain (Paris, France). Gridded filters of Alu-PCR products of the ICRF library and ICRF YACs were provided by Günther Zehetner at the Imperial Cancer Research Fund (London, U.K.). Gridded colony filters of the ICI library and YACs of the ICI and CEPH library were provided by the YAC Screening Center Leiden (The Netherlands, supported by NWO and the EU-grant PL930088). The hybrid cell line AM445x393 was kindly provided by Dr.H.H.Ropers. These studies were in part supported by de Nederlandse Organisatie voor Wetenschappelijk Onderzoek (NWO), de Nederlandse Vereniging ter Voorkoming van Blindheid, het Klinisch Genetisch Centrum Leiden (KGCL), the Medical Research Council (MRC) and the Wellcome Trust.

### **ABBREVIATIONS**

KFSD, keratosis follicularis spinulosa decalvans; RS, retinoschisis; CLS, Coffin-Lowry syndrome; HYP, hypophosphatemic rickets; SEDL, spondylo-epiphyseal dysplasia; RP15, X-linked dominant cone-rod degeneration (retinitis pigmentosa-15).

### **REFERENCES**

- 1 Cohen D, Chumakov I, Weissenbach J. A first generation physical map of the human genome. *Nature* 1993;366:698-701.
- 2 Gyapay G, Morissette J, Vignal A, Dib C, Fizames C, Millasseau P, Marc S, Bernardi G, Lathrop M, Weissenbach J. The 1993-94 Génethon human genetic linkage map. *Nature Genet* 1994;7:246-9.
- 3 Schlessinger D, Mandel J-L, Monaco AP, Nelson DL, Willard HF. Report and abstracts of the fourth international workshop on human X chromosome mapping 1993. *Cytogenet Cell Genet* 1993;64:147-94.
- 4 Poustka AM, Schlessinger D. Report of the Fifth International Workshop on Human X Chromosome Mapping 1994. Heidelberg, Germany; April 24-27. *Cytogenet Cell Genet* 1994;67:295-358.
- 5 McGuire RE, Sullivan LS, Blanton SH, Church MW, Heckenlively JR, Daiger SP.

- X-linked dominant cone-rod degeneration: linkage mapping of a new locus for Retinitis Pigmentosa (RP15) to Xp22.13-p22.11. *Am J Hum Genet* 1995;57:87-94.
- 6 Bergen AAB, Van Schooneveld MJ, Orth U, Bleeker-Wagemakers EM, Gal A. Multipoint linkage analysis in X-linked juvenile retinoschisis. *Clin Gen* 1993;43:113-6.
- 7 Bergen AAB, Ten Brink JB, Bleeker-Wagemakers LM, Van Schooneveld MJ. Refinement of the chromosomal position of the X-linked juvenile retinoschisis disease gene. *J Med Genet* 1994;31:972-5.
- 8 Oosterwijk JC, Nelen M, van Zandvoort PM, van Osch LDM, Oranje AP, Wittebol-Post D, Van Oost BA. Linkage analysis of Keratosis Follicularis Spinulosa Decalvans, and regional assignment to human chromosome Xp21.2-p22.2. *Am J Hum Genet* 1992;50:801-7.
- 9 Coffey AJ, Roberts RG, Green ED, Cole CG, Butler R, Anand R, Gianelli F, Bentley DR. Construction of a 2.6-Mb contig in yeast artificial chromosomes spanning the human dystrophin gene using an STS-based approach. *Genomics* 1992;12:474-84.
- 10 Alitalo T, Francis F, Kere J, Lehrach H, Schlessinger D, Willard HF. A 6-Mb YAC contig in Xp22.1-p22.2 spanning the DXS69E, XE59, GLRA2, PIGA, GRPR, CALB3 and PHKA2 genes. *Genomics* 1995;25:691-700.
- 11 Oosterwijk JC, Van der Wielen MJR, Van de Vosse E, Voorhoeve E, Bakker E. Refinement of the localisation of X-linked keratosis follicularis spinulosa decalvans (KFSD) gene in Xp22.1-p22.2. *J Med Genet* 1995;32:736-9.
- 12 Anand R, Riley JH, Butler R, Smith JC, Markham AF. A 3.5 genome equivalent multi access YAC library: construction, characterisation, screening and storage. *Nucleic Acids Res* 1990;18:1951-6.
- 13 Mohandas TK, Speed RM, Passage MB, Yen PH, Chandley AC, Shapiro LJ. Role of the pseudoautosomal region in sex-chromosome pairing during male meiosis: meiotic studies in a man with a deletion of distal Xp. *Am J Hum Genet* 1992;51:526-33.
- 14 Larin Z, Monaco AP, Lehrach H. Yeast artificial chromosome libraries containing large inserts from mouse and human DNA. *Proc Natl Acad Sci U S A* 1991;88:4123-7.
- 15 Breukel C, Wijnen J, Tops C, Van der Klift H, Dauwerse H, Meera Khan P. Vector-Alu PCR: a rapid step in mapping cosmids and YACs. *Nucleic Acids Res* 1990;18:3097
- 16 Donis-Keller H, Green P, Helms C, Cartinhour S, Weiffenbach B, Stephens K, Keith TP, Bowden DW, Smith DR, Lander ES, *et al.* A genetic linkage map of the human genome. *Cell* 1987;51:319-37.
- 17 Wapenaar MC, Petit C, Basler E, Ballabio A, Henke A, Rappold GA, Van Paassen HMB, Blonden LAJ, Van Ommen GJB. Physical mapping of 14 new DNA markers isolated from the human distal Xp region. *Genomics* 1992;13:167-75.
- 18 Aldridge J, Kunkel L, Bruns G, Tantravahl U, Lalande M, Brewster T, Moreau E, Wilson M, Bromley W, Roderick T, *et al.* A strategy to reveal high-frequency RFLPs along the human X chromosome. *Am J Hum Genet* 1984;36:546-64.
- 19 Stambolian D, Lewis RA, Buetow K, Bond A, Nussbaum R. Nance-Horan Syndrome: localization within the region Xp21.1-Xp22.3 by linkage analysis. *Am J Hum Genet* 1990;47:13-9.
- 20 Willard HF, Schmeckpeper BJ, Smith KD, Goss SJ. High resolution regional mapping of the human X chromosome by radiation induced segregation analysis of X-linked DNA probes. *Cytogenet Cell Genet* 1984;37:609-10.

- 21 Camerino G, Koenig M, Moisan JP, Oberle I, Morlé F, Jaye M, De la Salle H, Weil D, Hellkuhl B, Grzeschik KH, *et al.* Regional mapping of coagulation factor IX gene and of several unique DNA sequences on the human X chromosome. *Cytogenet Cell Genet* 1984;37:431-2.
- 22 Den Dunnen JT, Van Ommen G-JB. ; Mathew CG, editors. *Methods in Molecular Biology. Vol.9: Protocols in Human Molecular Genetics.* Clifton, New Jersey: Humana Press Inc. 1991; 17, Pulsed-Field Gel Electrophoresis. p. 169-82.
- 23 Dauwerse JG, Jumelet EA, Wessels JW, Saris JJ, Hagemeyer A, Beverstock GC, Van Ommen GJB. Extensive cross-homology between the long and the short arm of chromosome 16 may explain leukemic inversions and translocations. *Blood* 1992;79:1299-304.
- 24 Cole CG, Goodfellow PN, Bobrow M, Bentley DR. Generation of novel sequence tagged sites (STSs) from discrete chromosomal regions using Alu-PCR. *Genomics* 1991;10:816-26.
- 25 Holland J, Coffey AJ, Gianelli F, Bentley DR. Vertical integration of cosmid and YAC resources for interval mapping on the X-chromosome. *Genomics* 1993;15:297-304.
- 26 Condon GP, Brownstein S, Wang N-S, Kearns AF, Ewing CE. Congenital hereditary (juvenile X-linked) retinoschisis. *Arch Ophthalmol* 1986;104:576-83.
- 27 Schaefer L, Ferrero GB, Grillo A, Bassi MT, Roth EJ, Wapenaar MC, Van Ommen GJB, Mohandas TK, Rocchi M, Zoghbi HY, *et al.* A high resolution deletion map of human chromosome Xp22. *Nature Genet* 1993;4:272-9.
- 28 Chang Y-PC, Smith KD, Dover GJ. Dinucleotide repeat polymorphisms at the DXS85, DXS16 and DXS43 loci. *Hum Mol Genet* 1994;3:1029
- 29 Van de Vosse E, Booms PFM, Vossen RHAM, Wapenaar MC, Van Ommen GJB, Den Dunnen JT. A CA-repeat polymorphism near DXS418 (P122). *Hum Mol Genet* 1993;2:1202
- 30 Browne D, Barker D, Litt M. Dinucleotide repeat polymorphisms at the DXS365, DXS443 and DXS451 loci. *Hum Mol Genet* 1992;1:213
- 31 Rowe PSN, Goulding J, Read A, Lehrach H, Francis F, Hanauer A, Oudet C, Biancalana V, Kooh SW, Davies KE, *et al.* Refining the genetic map for the region flanking the X-linked hypophosphataemic rickets locus (Xp22.1-22.2). *Hum Genet* 1994;93:291-4.
- 32 Chumakov IM, Le Gall I, Billault A, Ougen P, Soularue P, Guillou S, Rigault P, Bui H, De Tand M-F, Barillot E, *et al.* Isolation of chromosome 21-specific yeast artificial chromosomes from a total human genome library. *Nature Genet* 1992;1:222-5.
- 33 Lehrach H, Drmanac R, Hoheisel J, *et al.* Davies KE, Tilghman SM, editors. *Genome analysis vol 1: Genetic and physical mapping.* Cold Spring Harbor: Cold Spring Harbor Laboratory Press, 1990;p. 39-81.
- 34 Monaco AP, Walker AP, Millwood I, Larin Z, Lehrach H. A yeast artificial chromosome contig containing the complete Duchenne muscular dystrophy gene. *Genomics* 1992;12:465-73.
- 35 Baldini A, Ross M, Nizetic D, Vatcheva R, Lindsay EA, Lehrach H, Siniscalco M. Chromosomal assignment of human YAC clones by fluorescence in situ hybridization: use of single-yeast-colony PCR and multiple labeling. *Genomics* 1992;14:181-4.
- 36 Wapenaar MC, Kievits T, Meera Khan P, Pearson PL, Van Ommen GJB. Isolation and characterization of cell hybrids containing human Xp-chromosome fragments. *Cytogenet*

- Cell Genet 1990;54:10-4.
- 37 Wieacker P, Davies KE, Cooke HJ, Pearson PL, Williamson R, Bhattacharya S, Zimmer J, Ropers H-H. Toward a complete linkage map of the human X chromosome: regional assignment of 16 cloned single-copy DNA sequences employing a panel of somatic cell hybrids. *Am J Hum Genet* 1984;36:265-76.
- 38 Baldini A, Ward DC. In situ hybridization banding of human chromosomes with Alu-PCR products: a simultaneous karyotype for gene mapping studies. *Genomics* 1991;9:770-4.
- 39 Green ED, Riethman HC, Dutchik JE, Olson MV. Detection and characterization of chimeric yeast artificial-chromosome clones. *Genomics* 1991;11:658-69.
- 40 Francis F, Rowe PSN, Econs MJ, Gee See C, Benham F, O'Riordan JLH, Drezner MK, Hamvas RMJ, Lehrach H. A YAC contig spanning the hypophosphatemic rickets disease gene (HYP) candidate region. *Genomics* 1994;21:229-37.
- 41 Weissenbach J, Gyapay G, Dib C, Vignal A, Morissette J, Millasseau P, Vaysseix G, Lathrop M. A second-generation linkage map of the human genome. *Nature* 1992;359:794-801.
- 42 Biancalana V, Trivier E, Weber C, Weissenbach J, Rowe PSN, O'Riordan JLH, Partington MW, Heyberger S, Oudet C, Hanauer A. Construction of a high-resolution linkage map for Xp22.1-p22.2 and refinement of the genetic localization of the Coffin-Lowry syndrome gene. *Genomics* 1994;22:617-25.

